UNIVERSITY OF TWENTE.

**Faculty of Electrical Engineering,
Mathematics & Computer Science**

State of the art LC-based frequency reference

Simon Busscher

B.Sc. Thesis
January 2019

Supervisors:
dr. ir. A.J. Annema
dr. ir. R.J.E. Hueting
MSc A.S. Delke

Integrated Circuit Design Group
Faculty of Electrical Engineering,
Mathematics and Computer Science
University of Twente
P.O. Box 217
7500 AE Enschede
The Netherlands

Abstract

De facto standard for frequency references is the crystal-based oscillator. While having decent frequency stability $(\pm 1ppm/^{O}C)$, it is let down by its cost and size. These are the reasons for switching to the LC-based cross-coupled CMOS-design which has the advantages of being cheaper and smaller, enabling on-chip implementation. However, in the 1 GHz frequency region the problem arises with the quality factor of inductors where $Q_L << Q_C$ and therefore $R_L >> R_C$. Variances in temperature will affect the resistances the most and R_L will therefore have the most influence in varying oscillation frequency as function of temperature. All the cross-coupled configurations suffer from these variations of R_L so it would be interesting to investigate various LC-architectures (like the Hartley or Clapp) to check how they are affected by R_L variations. The common-gate Colpitts oscillator was found out to be less affected by the parasitic resistance R_L and better temperature stable $(\pm 10ppm/^{O}C)$ than the widely-used cross-coupled LC-oscillator $(\pm 50ppm/^{O}C)$.

In this report, the frequency stability as a result of temperature variations of various common-gate oscillator designs in the 1 GHz region are calculated and simulated and compared to the common-gate Colpitts oscillator frequency stability in order to find a better performing configuration. The configurations that are tested include Hartley, Clapp and a cross-coupled LC-oscillator with extra capacitor. Furthermore, adaptations to the Colpitts design are calculated where one design has a parallel capacitor added to the inductor to tune the inductor and the other one a series resistance added to the capacitors in order to tune the Q_C.

Results show that the Hartley, Clapp and cross-coupled $+Ca$ are not better performing than the original Colpitts in terms of frequency stability. Both the adapted Colpitts designs however show significant improvement in the simulations when tuned right $(\pm 100ppm\ \Delta 100^{O}C)$.

Contents

Chapter 1

Introduction

In this section the motivation is given containing the background information as well as a problem definition. The goal of the research is formulated in the research question.

1.1 Motivation

De facto standard for frequency references is the crystal-based (XO) oscillator [1]. While having having decent frequency stability $(\pm 1ppm/^{O}C)$, it is let down by its cost and size. Considering these pitfalls, the trend is to use a CMOS-based cross-coupled LC-oscillator which are low in cost and fully chip-integrable. The oscillation frequency of the cross-coupled type design [2] contains however a large contribution of parasitic resistance coming from the inductive impedance in the 1 GHz range, since $Q_L << Q_C$ and therefore $R_L >> R_C$ [1]. Variances in temperature will affect the resistances the most and R_L will therefore have the most influence in varying oscillation frequency as function of temperature. This causes the cross-coupled stability to be set at $(\pm 50ppm/^{O}C)$ [3]. Because of this deviation caused by the large influence of R_L, other LC oscillator configurations can be explored that may be less affected by R_L. The Colpitts oscillator was found out to be less affected by the parasitic resistance R_L [4].

The Colpitts configuration [4] already has good prospects of being used as fundamental for a temperature stable oscillator in the range of 1 GHz $(\pm 10ppm/^{O}C)$. Possibly with temperature stability that can compete with the temperature stability performance from XO $(\pm 1ppm/^{O}C)$ and silicon MEMS resonators $(\pm 20ppm/^{O}C)$ [1] [2]. Especially cost, size, and in some degree jitter are factors at which the LC-based oscillator scores well in comparison [1] [5]. However, there are more LC-based configurations available with structures comparable to the Colpitts structure like Hartley or Clapp oscillators. Suspicion would assume that systems which are less reliant

on inductive components, and which will therefore less dependent on the R_L term, would probably have good prospects. However, the fundamentals for oscillation still need to be satisfied[1]. By comparing the results of the other LC-configurations to the results of the Colpitts, it can be determined how stable the new configuration is compared to the Colpitts. Furthermore, simulations need to be done in order to confirm the performance of the new systems.

1.2 Research question

The goal of this report is to find an oscillator configuration among the listed LC-oscillator configurations that can achieve better temperature stability than the Colpitts oscillator in the 1 GHz frequency region. If none of the listed solutions provide a stability performance increase over the Colpitts, the Colpitts would enhance its position. Eventual successful attempts will be confirmed by further calculations and simulations. Both successful and unsuccessful attempts will be evaluated and documented.

Chapter 2

LC oscillators

This chapter will represent the various LC oscillators of which the oscillation frequencies and temperature stabilities are calculated and simulated. In the comparison chapter, the different configurations are compared side by side in order to gather knowledge how the configurations perform with respect to the Colpitts oscillator in terms of frequency stability.

2.1 LC-oscillator configuration

All oscillator configurations are based on the Colpitts common-gate structure as used by Alexander Delke [4], shown in Figure B.1. The same common-gate configuration is used as basis for the other LC-oscillators which can be derived by filling in the corresponding impedances in Figure B.1 where (a) includes the MOSFET driver which is assumed linear and ideal in (b) which is used for the derivations (except for the cross-coupled $(+Ca)$ configuration where the simplified schematic is B.2). The corresponding configurations will be placed in Appendix B and will be referred to if needed in during calculations in section 2.2.

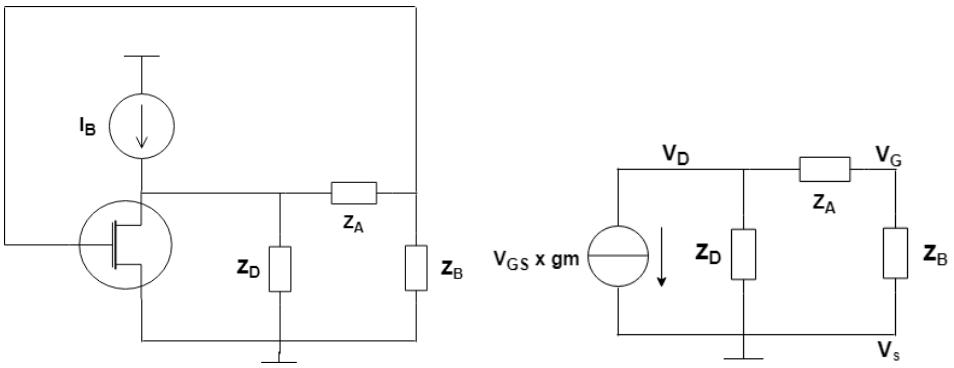

Figure 2.1: The common-gate configuration

2.2 Calculations for ω and stability

Before deriving the temperature coefficients of the circuits, the oscillation frequencies need to be determined. For every oscillating circuit, the Barkhausen criteria [4] need to be met. The oscillation frequency of the oscillator can therefore be derived from the criterion $Im(AB) = 0$ which states that the total reactive power of the closed-loop oscillator circuit needs to be 0. For the common-gate configuration of Figure 2.1 it is derived in [4] that equation 2.1 needs to be met.

$$\sum X = -(\frac{1}{Q_B} + \frac{1}{Q_D}) \sum R \tag{2.1}$$

The $\sum X$ term is the sum of all reactances in the circuit whereas the $\sum R$ is the sum of all resistances and Q_B and Q_D are the quality factors of the corresponding impedances defined by $Q = \frac{X}{R}$[1].

For every configuration, the equation 2.1 can be filled in which will therefore be used as starting point for the oscillation frequency calculation of a certain configuration. During derivations, the assumption $\omega \approx \omega_0$ (2.2) is sometimes made for simplification purposes where ω_0 is the product of purely reactive components.

$$\omega_O = \sqrt{\frac{1}{L_{tot} C_{tot}}} \tag{2.2}$$

After having determined the oscillation frequency of a circuit, the frequency deviation over temperature as a result of the temperature coefficients of present components. For every component, the influence on frequency is determined. For a certain component A it is done according to equation 2.3 [1].

$$f_{TC,A} = \frac{\partial \omega}{\partial A} \frac{\partial A}{\partial T} \frac{1}{\omega} \tag{2.3}$$

The $\frac{\partial \omega}{\partial A}$ is component and system independent whereas $\frac{\partial A}{\partial T} = \frac{\partial}{\partial T} A_{const}(1 + a_{TC,A} T) = a_{TC,A} A$ [1][2] which is the variation of the component value over temperature. Since the system only contains inductors and capacitors with their corresponding parasitic resistances, the total frequency deviation of a circuit with respect to temperature is the sum of all individual components contributing to the frequency deviation as can be seen in equation 2.4.

$$f_{TC,tot} = f_{TC,R_L} + f_{TC,R_C} + f_{TC,L} + f_{TC,C} \tag{2.4}$$

For all derivations, the parameters of table B.1 were taken into account as well as $R_L >> R_C$ [1] for the given frequency range.

[1] X is the imaginary part and R the real part of the respective impedance

[2] assumed constant with first order temperature dependency

2.2.1 Hartley

Starting with the Hartley configuration as seen in Appendix B.3, the oscillation frequency is derived first following the derivation steps in Appendix A equation A.1, where $L = L_B + L_D$ and $R_L = R_B + R_D$.

$$\omega \approx \sqrt{\frac{1}{LC}}\sqrt{\frac{L - 2CR_L^2}{L}} \tag{2.5}$$

What immediately stands out is the presence of a R_L^2 term. Based on the oscillation frequency of equation 2.5, the various f_{TC}'s are derived in the Appendix A A.2 derivation where the $f_{TC,tot}$ is given in equation 2.6.

$$f_{TC,tot} = -\frac{2a_{TC,R_L}}{Q_L^2} - \frac{a_{TC,R_C}}{Q_L Q_C} - \frac{a_{TC,L}}{2} - \frac{a_{TC,C}}{2} \tag{2.6}$$

What stands out here is that all temperature coefficients seem to have a negative effect on the total f_{TC}.

2.2.2 Clapp

Moving over to the Clapp configuration as seen in Appendix B.4, the oscillation frequency is derived following the derivation steps in Appendix A equation A.3, where $C = C_{series} = \frac{C_A C_B C_D}{C_A C_B + C_A C_D + C_B C_D}$, $R_A \approx R_L$ and $R_C \approx R_B + R_D$.

$$\omega \approx \sqrt{\frac{1}{LC}}\sqrt{\frac{L + 2CR_C R_L}{L}} \tag{2.7}$$

Based on the oscillation frequency of equation 2.7, the various f_{TC}'s are derived in Appendix A derivation A.4 where the $f_{TC,tot}$ is given in equation 2.8. During simplifications, it is assumed that all capacitors have the same Q_C term. Therefore, terms like $C_B R_B$ can be written as CR_C.

$$f_{TC,tot} = \frac{a_{TC,R_L}}{Q_L Q_C} + \frac{a_{TC,R_C}}{Q_L Q_C} - \frac{a_{TC,L}}{2} - \frac{a_{TC,C}}{2} \tag{2.8}$$

Both the calculated oscillation frequency and the f_{TC} appear to describe the same system as the Colpitts common-gate following Alexander's derivations [4]. It can therefore be assumed that the Clapp and the Colpitts configuration will have the same temperature dependent oscillation frequency.

2.2.3 Cross-coupled $(+Ca)$

The ordinary cross-coupled oscillator only includes a Z_B and a Z_D. In this case, an extra impedance Z_A is added instead of the usual short (Appendix Figures B.2, B.5).

The oscillation frequency is derived in Appendix A derivation A.5 and represented in equation 2.9. Here it is assumed that $C = \frac{C_A C_D}{C_A + C_D}$ and $R_C = R_A + R_D$

$$\omega \approx \sqrt{\frac{1}{LC}} \sqrt{\frac{L - CR_L^2}{L}} \tag{2.9}$$

The f_{TC}'s are derived in Appendix A, derivation A.6. The $f_{TC,tot}$ is given in equation 2.10. Like with the Clapp derivations, it was assumed that all capacitors share the same Q_C, making it possible to write terms like $C_B R_B$ as CR_C.

$$f_{TC,tot} = -\frac{a_{TC,R_L}}{Q_L^2} + \frac{a_{TC,R_C}}{Q_C^2} - \frac{a_{TC,L}}{2} - \frac{a_{TC,C}}{2} \tag{2.10}$$

Also for the cross-coupled $(+Ca)$ it seems that the oscillation frequency as well as the f_{TC} appears to be similar to the standard cross-coupled design [2]. It might be assumed that the oscillation frequency of both systems will have the same temperature dependency.

2.2.4 Colpitts $(+Ca)$

In this section, a tuned variant of the original Colpitts is derived. This is done by adding a capacitor C_A parallel to the inductor L_A as seen in Appendix B.6. Since $Q_L << Q_C$, the resistance of capacitor C_A can be neglected and the new impedance Z_A is shown in equation 2.11.

$$Z_A \approx \frac{R_L + j\omega L}{1 + R_L j\omega C_A - \omega^2 L C_A} \tag{2.11}$$

Also the new R_A and X_A can be derived as $R_A = Re\{Z_A\}$ and $X_A = Im\{Z_A\}$ which is done in Appendix A derivation A.7 and A.8 where $C = \frac{C_B C_D}{C_B + C_D}$.

$$R_A \approx R_L \frac{C^2}{(C_A - C)^2} \qquad X_A \approx \omega L \frac{C}{(C - C_A)} \tag{2.12}$$

These new terms (2.12) can be written into inductor parameters with a scalar in front defined by equations 2.13.

$$A_r = \frac{C^2}{(C_A - C)^2} \qquad A_X = \frac{C}{(C - C_A)} \tag{2.13}$$

This translates to $R_A = A_R R_L$ and $X_A = A_X \omega L$ which helps deriving the oscillation frequency and frequency deviation since both R_A and X_A are written as the inductor components of the standard Colpitts configuration with an extra scalar. The other thing to take into account is that the ω_0 changes as well. This is due to the new definition of X_A where the new ω_0 is given in equation 2.14 as a result of derivation A.9.

$$\omega_0 = \sqrt{\frac{1}{A_X LC}} \tag{2.14}$$

With the use of all new determined parameters, the extended oscillation frequency (2.15) can be determined as done in Appendix A derivation A.10, where $R_C = R_B + R_D$

$$\omega = \sqrt{\frac{1}{A_X LC}}\sqrt{\frac{A_X L + 2CR_C A_R R_L}{A_X L}} \tag{2.15}$$

Corresponding to 2.15, the f_{TC} values are derived in Appendix A A.11 resulting in 2.16. It can be noted that only the positive f_{TC,R_L} and f_{TC,R_C} are affected by A_X and A_R, giving the opportunity to compensate for the negative coefficients by tuning A_X and A_R

$$f_{TC,tot} = \frac{A_R a_{TC,R_L}}{A_X Q_L Q_C} + \frac{A_R a_{TC,R_C}}{A_X Q_L Q_C} - \frac{a_{TC,L}}{2} - \frac{a_{TC,C}}{2} \tag{2.16}$$

However, a mismatch was discovered when comparing the calculated and simulated f_{TC} values. The problem was traced down to the definition of A_X. The R_L terms in the derivation of X_A (A.8) fell out during simplification. Therefore, a new A_X was defined (derived in Appendix A A.12) and introduced as component susceptible to temperature changes due to R_L, influencing the temperature dependent oscillation frequency.

$$f_{TC,A_X} = \frac{\partial\omega}{\partial T}\frac{1}{\omega} = \frac{\partial\omega}{\partial A_X}\frac{\partial A_X}{\partial R_L}\frac{\partial R_L}{\partial T}\frac{1}{\omega} \tag{2.17}$$

The additional f_{TC,A_X} as defined by 2.17 is derived in Appendix A A.13 resulting in equation 2.18.

$$f_{TC,A_X} = \frac{2a_{TC,R_L} C_A C^3 R_L^2 (C_A - C)(2C_A^2 - 2C_A C + C^2)}{L(C_A^2 - C_A C + C^2)^3} \tag{2.18}$$

Now the total frequency deviation results in equation 2.19.

$$f_{TC,tot} = \frac{A_R a_{TC,R_L}}{A_X Q_L Q_C} + \frac{A_R a_{TC,R_C}}{A_X Q_L Q_C} - \frac{a_{TC,L}}{2} - \frac{a_{TC,C}}{2} + f_{TC,A_X} \tag{2.19}$$

2.2.5 Colpitts with tuned Q-factor

The last configuration is basically the same as the original common-gate Colpitts (Figure B.1). Whereas the f_{TC} is given by 2.22, it can be rewritten in a form for Q_L or Q_C where $f_{TC} = 0$ holds, such that the positive coefficients compensate the negative coefficients. This is done in Appendix A derivation A.14, resulting in equations 2.20.

$$f_{TC,tot} = \frac{a_{TC,R_L}}{Q_L Q_C} + \frac{a_{TC,R_C}}{Q_L Q_C} - \frac{a_{TC,L}}{2} - \frac{a_{TC,C}}{2} \tag{2.20}$$

$$\frac{a_{TC,R_L}}{Q_L Q_C} + \frac{a_{TC,R_C}}{Q_L Q_C} = \frac{a_{TC,L}}{2} + \frac{a_{TC,C}}{2} \tag{2.21}$$

$$Q_L = \frac{2(a_{TC,R_L} + a_{TC,R_C})}{Q_C(a_{TC,L} + a_{TC,C})} \quad Q_C = \frac{2(a_{TC,R_L} + a_{TC,R_C})}{Q_L(a_{TC,L} + a_{TC,C})} \tag{2.22}$$

This shows that one of the two Q-factors can be altered in order to achieve a theoretical, first-order solution of $f_{TC} = 0$, where the negative coefficients are exactly compensated. By filling in the values for the temperature coefficients and the correspondig Q-values, a new Q_L and Q_C is calculated. This states that either $Q_L new = 2.67$ or $Q_C new = 53.4$ can be used to compensate and achieve $f_{TC} = 0$, while the other Q-factor remains the same. This reduction in Q-factor can be easily achieved by multiplying the corresponding resistance by the downscaling factor which is 3.75 for both Q-values. This translates to multiplying resistance with a factor 3.75 since $Q_L = \frac{\omega L}{R_L}$ and $Q_C = \frac{1}{\omega C R_C}$. The total Q-factor of the system [4] however, given in equation 2.23, needs to be as little affected as possible.

$$\frac{1}{Q_T} = \omega C \sum R = \omega C (R_L + R_C) \tag{2.23}$$

Since $R_L >> R_C$, multiplying R_C with 3.75 will give the smallest decrease in Q_T. Therefore, the new Q_C is set at 53.4.

2.2.6 Comparison of calculated f_{TC} coefficients

In this section an f_{TC} breakdown is represented of all configurations for side-by-side comparison. The tables are split in mixed configurations (Table 2.1) and tuned Colpitts configurations (Table 2.2).

Table 2.1: Temperature coefficients of the various LC-configurations

	Cross-coupled	**Colpitts**	**Hartley**	**Clapp**	**Cross-coupled** $(+Ca)$
$f_{TC,L}$	$\frac{-\alpha_L}{2}$	$\frac{-\alpha_L}{2}$	$\frac{-\alpha_L}{2}$	$\frac{-\alpha_L}{2}$	$\frac{-\alpha_L}{2}$
$f_{TC,C}$	$\frac{-\alpha_C}{2}$	$\frac{-\alpha_C}{2}$	$\frac{-\alpha_C}{2}$	$\frac{-\alpha_C}{2}$	$\frac{-\alpha_C}{2}$
f_{TC,R_L}	$\frac{-\alpha_{R_L}}{\mathbf{Q_L^2}}$	$\frac{\alpha_{R_L}}{\mathbf{Q_L Q_C}}$	$\frac{-2\alpha_{R_L}}{\mathbf{Q_L^2}}$	$\frac{\alpha_{R_L}}{\mathbf{Q_L Q_C}}$	$\frac{-\alpha_{R_L}}{\mathbf{Q_L^2}}$
f_{TC,R_C}	$\frac{\alpha_{R_C}}{\mathbf{Q_C^2}}$	$\frac{\alpha_{R_C}}{\mathbf{Q_L Q_C}}$	$\frac{-\alpha_{R_C}}{\mathbf{Q_L Q_C}}$	$\frac{\alpha_{R_C}}{\mathbf{Q_L Q_C}}$	$\frac{\alpha_{R_C}}{\mathbf{Q_C^2}}$

When observing Table 2.1, it appears that for all configurations the $f_{TC,L}$ and $f_{TC,C}$ are the same. More similarities are discovered for the f_{TC,R_L} and f_{TC,R_C} when comparing the Colpitts to the Clapp as well as the cross-coupled to the cross-coupled $(+Ca)$. It suggest that these configurations will give the same frequency stability performance which will be checked in the simulations. The Hartley configuration however seems to be the only one with a unique f_{TC,R_L} and f_{TC,R_C}. A possible problem might be predicted since all Hartley's coefficients are negative. Also the $f_{TC,R_L} = \frac{-2\alpha_{R_L}}{\mathbf{Q_L^2}}$ term is very influential considering Table B.1 and Table B.2.

In Table 2.2, the temperature coefficients for the original Colpitts and Colpitts $(+Ca)$ are displayed. It can be observed that the additional A_X, A_R and f_{TC,A_X} can be used to tweak the positive coefficients in order to compensate for the negative coefficients

Table 2.2: Temperature coefficients of the Colpitts and Colpitts $(+Ca)$ configurations

	Colpitts	**Colpitts** $+(Ca)$
$f_{TC,L}$	$\frac{-\alpha_L}{2}$	$\frac{-\alpha_L}{2}$
$f_{TC,C}$	$\frac{-\alpha_C}{2}$	$\frac{-\alpha_C}{2}$
f_{TC,R_L}	$\frac{\alpha_{R_L}}{\mathbf{Q_L Q_C}}$	$\frac{A_R \alpha_{R_L}}{A_X \mathbf{Q_L Q_C}} + f_{TC,A_X}$
f_{TC,R_C}	$\frac{\alpha_{R_C}}{\mathbf{Q_L Q_C}}$	$\frac{A_R \alpha_{R_C}}{A_X \mathbf{Q_L Q_C}}$

2.3 Simulations for frequency stability

In this part of the report, simulations are conducted. The phase ($Im\{AB\}$) of the closed loop oscillator circuit (asssuming ideal and linear MOSFET) is plotted for the temperatures $-40^O C$, $30^O C$ and $150^O C$ across the frequency spectrum in a phase plot.

Based on the frequency values at which $Im\{AB\} = 0$ for the given temperature range, the frequency deviation is derived and represented in parts per million (ppm). This is plotted across temperature together with the calculated frequency deviation of the given system. The simulated and calculated values are normalised for $30^O C$.

All simulations are conducted in MATLAB and the parameter ranges, values and temperature coefficients defined in the tables B.1 and B.2 are used.

2.3.1 Hartley

First, the two plots are made for the Hartley.

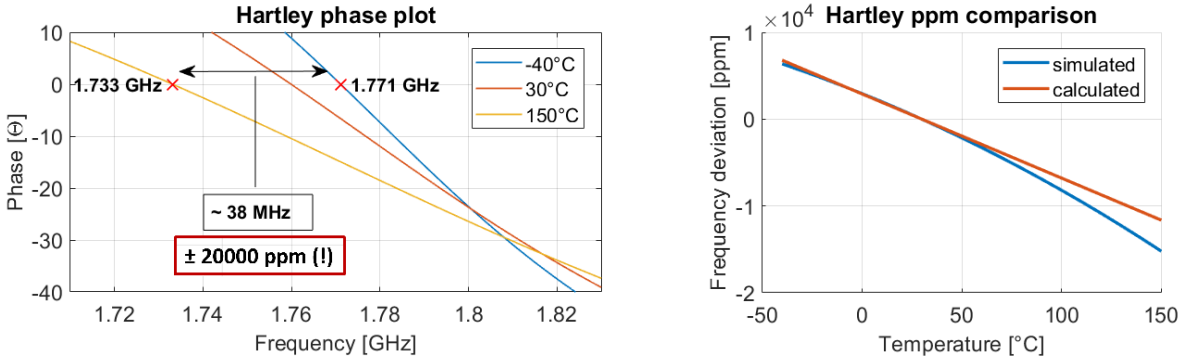

(a) (b)

Figure 2.2: Hartley simulation results

From Figure2.2 (a), it can be derived that the maximum deviation is $38MHz$ or $20,000ppm$. This can also be conducted from (b). What also stands out is that the phase intersection for the given temperatures is approximately -30^O. Figure (b)

also nicely shows how the calculations are a first order approximation (at normalised temperature) of a slighter higher order system. As expected from the calculations, all the calculated negative temperature coefficients are heavily degrading the oscillation frequency for an increasing temperature.

2.3.2 Clapp

The same simulations are run for the Clapp configuration.

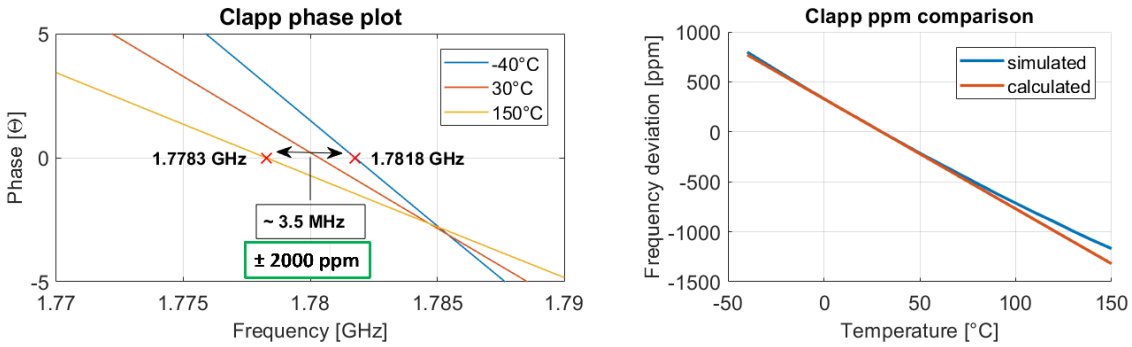

(a) (b)

Figure 2.3: Clapp simulation results

In Figure2.3 (a), it can be seen that the given deviation is around $3,5MHz$ or $2,000ppm$. Here the phase intersection for the temperatures is around -3^O. Also here, the calculated frequency deviation in Figure2.3 (b) corresponds quite decently with the higher order simulation. From these results it can be deduced that the system has got the same frequency behaviour as the Colpitts over temperature.

2.3.3 Cross-coupled $(+Ca)$

The simulations are also done for the cross-coupled $(+Ca)$ configuration.

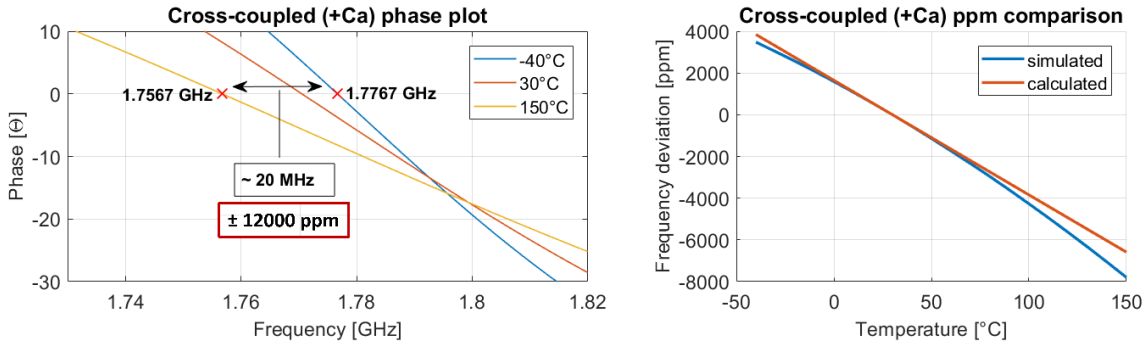

(a) (b)

Figure 2.4: Cross-coupled $(+Ca)$ simulation results

In Figure2.4 (a), it can be seen that the maximum deviation is around $20MHz$ or $12,000ppm$. Here the phase intersection for the temperatures is around -18^O out of phase. Also for the cross-coupled $(+Ca)$, the calculated frequency deviation in Figure2.4 (b) shows similarities to the higher order simulation. It seems that the extra added C_A only affects the oscillation frequency since the temperature behaviour is comparable to that of the original cross-coupled configuration.

2.3.4 Colpitts $(+Ca)$

In this section, simulations are done for the Colpitts $(+Ca)$ for three different C_A values. The first simulations are run with $C_A = 0$, the second with $C_A = 560fF$ and the third with $C_A = 1120fF$.

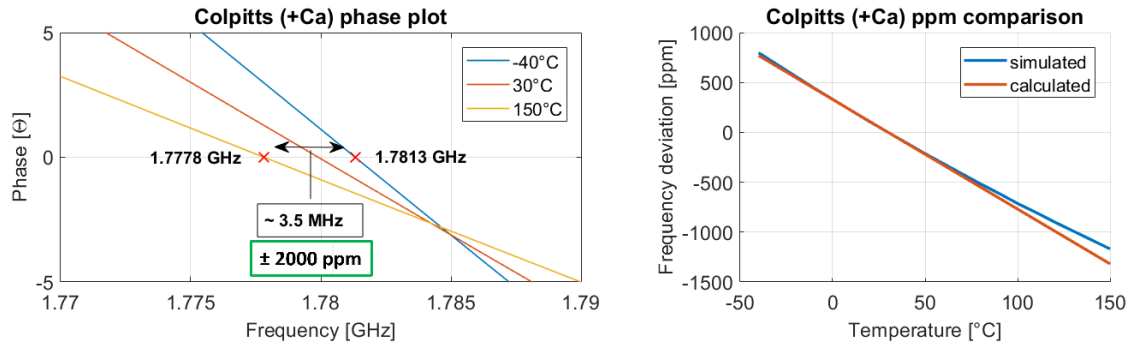

(a) (b)

Figure 2.5: Colpitts $C_A = 0$ simulation results

When $C_A = 0$, the oscillator configuration basically turns back into an ordinary Colpitts oscillator. By observing the results from Figure 2.5, these similarities can be seen since the total deviation here is $3,5MHz$ or $2,000ppm$. The temperature

intersection seems to be -3^O out of phase. The results from both calculations and simulations are also in agreement with eachother.

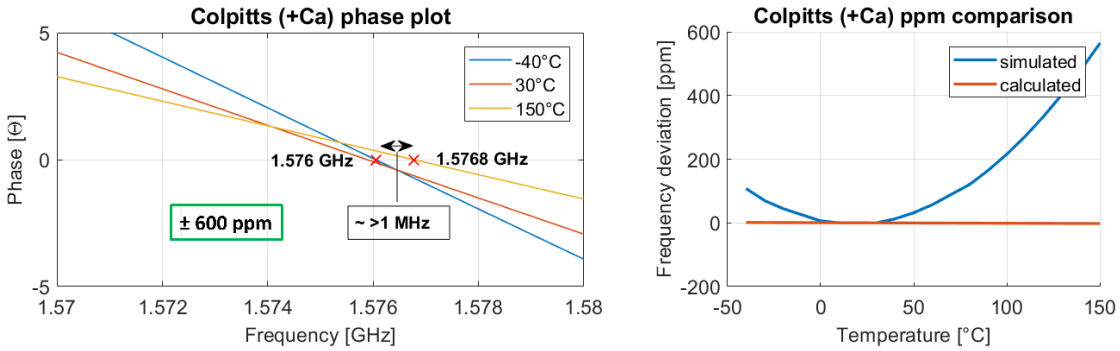

(a) (b)

Figure 2.6: Colpitts $C_A = 560fF$ simulation results

The interesting results come when the (C_A) value is tuned to let the expression of 2.19 go to zero. The value $C_A = 560fF$ is used in the simulations of Figure 2.6. While the first order approximation of the calculations result in $f_{TC} = 0$, the simulations result in a parabolic shape. Since the frequency behaviour as a result of temperature is not strictly linear, the temperature intersection, which seems to be at around a phase of 0^O, is not a single point but more or less a triangle shaped intersection. The calculations appear to formulate a tangent line of the parabolic shape for the normalised temperature value. The frequency deviation numbers of $\sim> 1MHz$ or $600ppm$ seem to be quite impressive. What seems to be more impressive is that ($\sim 100ppm\ \Delta \pm 50^OC$) can be achieved for the tuned for temperature. Also the effect of A_X on the overall oscillation frequency (2.14) can be duly noted.

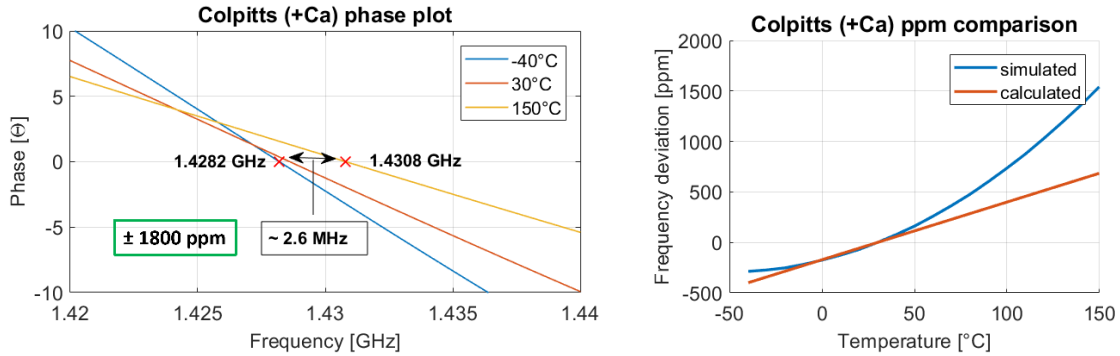

(a) (b)

Figure 2.7: Colpitts $(C_A) = 1120fF$ simulation results

In Figure 2.7 the results for overshooting the value of C_A are presented. The frequency deviation slope is moving up as a result of the positive terms for the f_{TC}

in equation 2.16 taking over. This can also be seen by looking at the temperature intersection which is phase shifted to around 3^O. The total deviation in this case is approximately $\sim 2,6MHz$ or $1800ppm$.

2.3.5 Colpitts $(Qc = 53.4)$

At last the original Colpitts with tuned R_C values is simulated and checked.

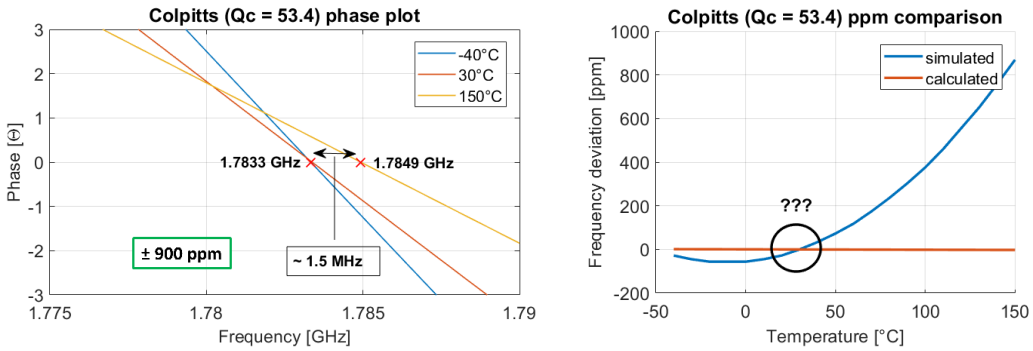

(a) (b)

Figure 2.8: Colpitts with tuned Q-factor

By looking at Figure 2.8 (b), a mismatch between the calculated and simulated f_{TC} values arises. This is due to the effect of having R_C increased in such a manner that $R_L >> R_C$ does not hold anymore which is assumed for simplification during f_{TC} derivations.

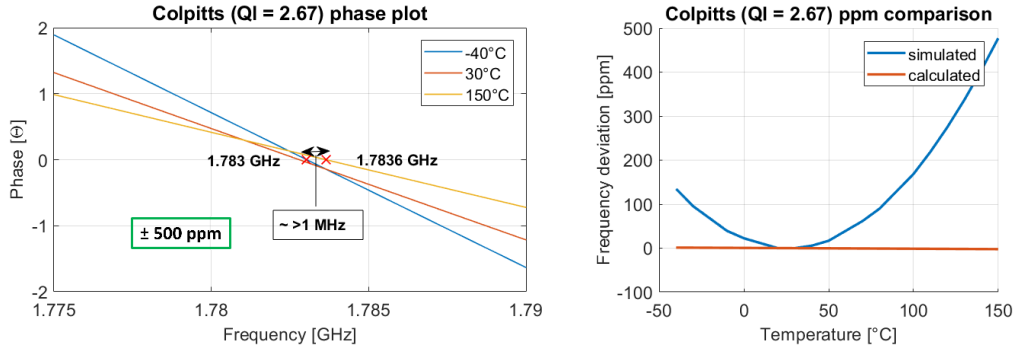

(a) (b)

Figure 2.9: Colpitts $(Q_L = 2.67)$ simulation results

For a proof of concept, Q_L is tuned in order to maintain $R_L >> R_C$ (and even more). Figure 2.9 gives a good representation of the concept and with a total deviation of $\sim> 1MHz$ or $500ppm$. By observing Figure 2.9 (b) at around the tuned for temperature, the total deviation over 100^OC (-20^OC to 80^OC) stays within the $100ppm$ deviation which translates to an impressive $1ppm/^OC$.

2.3.6 Comparison of simulated f_{TC} coefficients

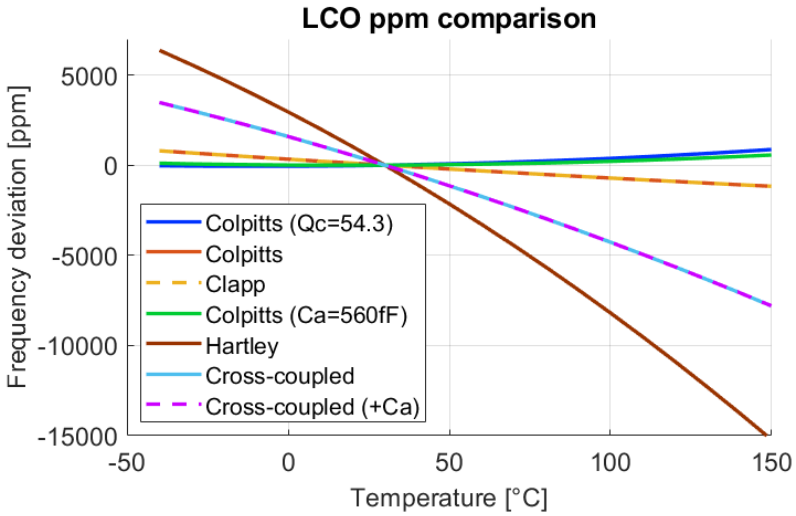

Figure 2.10: Frequency deviation comparison of all configurations

By looking at Figure 2.10, a division can be made between better performing configurations and worse performing configurations compared to the Colpitts. The Hartley has got the largest frequency deviation over temperature, followed by the two cross-coupled designs. The Clapp seems to perform the same as the original Colpitts. These configurations perform subpar or equal. However, the altered Colpitts designs show a performance increase over the original.

Chapter 3

Conclusion and discussion

In this part the conclusion is drawn based on previous found results. Based on the conclusion, a discussion is given where improvements and possible next steps are formulated.

3.1 Conclusion

Based on the results it can be concluded that there are possible configurations that are an improvement over the original Colpitts construction in terms of frequency stability over temperature. Both the Colpitts $(+Ca)$ and the Colpitts $(Q_C = 53.4)$ show quite a performance increase $(\pm 3ppm/^OC)$ compared to the standard Colpitts $(\pm 10ppm/^OC)$. The Clapp seems to perform equally to the Colpitts so adding the extra C_A component is not justified, at least according to the conducted calculations and simulations. The Hartley and cross-coupled $(+Ca)$ configurations have equal or subpar performance in terms of frequency stability.

3.2 Discussion

Although the results seem promising for the improved configurations, it is still uncertain how they cope with added parasitics and non-idealities coming from the MOSFET, supply and production processes. Also the effect of a load attached needs to be considered. Further simulations need to be conducted in order to check if the calculated approximations still hold. Also the robustness of the new configurations can be checked in comparison with the other LC-combinations to see if there is still a performance increase.

The research question for further research could be: How do the new configurations hold up when parasitics, non-idealities and other production variables are involved?

Bibliography

[1] P. H. Andrea Baschirotto, Ko A.A. Makinwa, *Frequency References, Power Management for SoC, and Smart Wireless Interfaces*. Springer International Publishing Switzerland, pp. 16-22, 2014.

[2] M. S. McCorquodale, *A 25-MHz Self-Referenced Solid-State Frequency Source Suitable for XO-Replacement*, pp. 943-946, May 209, vol. 56, no. 5.

[3] A. Ahmed, *A Highly Stable CMOS Self-Compensated Oscillator (SCO) Based on an LC Tank Temperature Null Concept*. Timing Products Division, Si-Ware Systems, Cairo, Egypt.

[4] J. Groszkowski, *Frequency of Self-Oscillations*. PWN - POLISH SCIENTIFIC PUBLISHERS · WARSZAW, 1964, -In accordance with the Colpitts common-gate calculations of Alexander Delke-, pp. 224-230.

[5] M. S. McCorquodale and V. Gupta, *A History of the Development of CMOS Oscillators: The Dark Horse in Frequency Control*. Silicon Frequency Control, Integrated Device Technology, May 2011.

Appendix A

Calculations for ω and f_{TC}

This part of the Appendix includes the extensive calculations and derivations.

A.1 Hartley oscillator

A.1.1 Oscillation frequency

$$\sum X = -(\frac{1}{Q_B} + \frac{1}{Q_D}) \sum R$$

$$-\frac{1}{\omega C_A} + \omega L_B + \omega L_D = -(\frac{R_B}{\omega L_B} + \frac{R_D}{\omega L_D})(R_A + R_B + R_D)$$

$$-\frac{1}{\omega C_A} + \omega L = -(\frac{R_B}{\omega L_B} + \frac{R_D}{\omega L_D})(R_A + R_B + R_D)$$

$$\frac{\frac{\omega^2}{\omega_0^2} - 1}{\omega C_A} = -(\frac{R_B}{\omega L_B} + \frac{R_D}{\omega L_D})(R_A + R_B + R_D)$$

$$\omega^2 = \omega_0^2(1 - \omega C(\frac{R_B}{\omega L_B} + \frac{R_D}{\omega L_D})(R_A + R_B + R_D))$$

$$\omega^2 = \frac{1}{LC}(1 - C(\frac{R_B}{L_B} + \frac{R_D}{L_D})(R_A + R_B + R_D)) \tag{A.1}$$

$$\omega^2 = \frac{1}{LC}(1 - C(\frac{R_B L_D}{L_B L_D} + \frac{R_D L_B}{L_B L_D})(R_A + R_B + R_D))$$

$$\omega^2 = \frac{1}{LC}(\frac{L_B L_D - C(R_B L_D + R_D L_B)(R_A + R_B + R_D)}{L_B L_D})$$

$$\omega^2 = \frac{1}{LC}(\frac{\frac{1}{4}L^2 - \frac{1}{2}LC(R_C + R_L)}{\frac{1}{4}L^2})$$

$$\omega = \sqrt{\frac{1}{LC}}\sqrt{\frac{L - 2CR_L(R_C + R_L)}{L}}$$

$$\omega = \sqrt{\frac{1}{LC}}\sqrt{\frac{L - 2CR_L^2}{L}}$$

A.1.2 Frequency stability

$$
\begin{aligned}
&\frac{\partial \omega}{\partial R_L} = -\frac{2C^2 R_L \omega_0^3}{\sqrt{-\frac{2CR_L^2}{L}+1}} \approx 2C^2 R_L \omega_0^3 \\
&\frac{\partial R_L}{\partial T} = a_{TC,R_L} R_L \\
&f_{TC,R_L} = \frac{\partial \omega}{\partial T}/\omega = \frac{\partial \omega}{\partial R_L}\frac{\partial R_L}{\partial T}/\omega \\
&= 2a_{TC,R_L} C^2 R_L^2 \omega_0^2 = \frac{2a_{TC,R_L} C^2 L^2 \omega_0^4}{Q_L^2} = \frac{2a_{TC,R_L}}{Q_L^2} \\
&\frac{\partial \omega}{\partial R_C} = -\frac{C^2 R_L \omega_0^3}{\sqrt{-\frac{2CR_L R_C}{L}+1}} \approx C^2 R_L \omega_0^3 \\
&\frac{\partial R_C}{\partial T} = a_{TC,R_C} R_C \\
&f_{TC,R_C} = \frac{\partial \omega}{\partial T}/\omega = \frac{\partial \omega}{\partial R_C}\frac{\partial R_C}{\partial T}/\omega \\
&= a_{TC,R_L} C^2 R_L R_C \omega_0^2 = \frac{a_{TC,R_C} R_C C^2 L \omega_0^3}{Q_L} = \frac{a_{TC,R_C} R_C C \omega_0}{Q_L} = \frac{a_{TC,R_C}}{Q_L Q_C} \\
&\frac{\partial \omega}{\partial L} = -\frac{(-4CR_L^2 + L)\omega_0}{2L^2\sqrt{-\frac{2CR_L^2}{L}+1}} = -\frac{L\omega_0}{2L^2} = -\frac{\omega}{2L} \\
&\frac{\partial L}{\partial T} = a_{TC,L} L \\
&f_{TC,L} = \frac{\partial \omega}{\partial T}/\omega = \frac{\partial \omega}{\partial L}\frac{\partial L}{\partial T}/\omega = -\frac{a_{TC,L} L}{2L} = -\frac{a_{TC,L}}{2} \\
&\frac{\partial \omega}{\partial C} = -\frac{L\omega_0^3}{2\sqrt{-\frac{2CR_L^2}{L}+1}} \approx -\frac{L\omega_0^3}{2} \\
&\frac{\partial C}{\partial T} = a_{TC,C} C \\
&f_{TC,C} = \frac{\partial \omega}{\partial T}/\omega = \frac{\partial \omega}{\partial C}\frac{\partial C}{\partial T}/\omega = -\frac{a_{TC,C} LC\omega^2}{2} = -\frac{a_{TC,C}}{2}
\end{aligned}
\tag{A.2}
$$

A.2 Clapp

A.2.1 Oscillation frequency

$$
\begin{aligned}
&\sum X = -(\frac{1}{Q_B} + \frac{1}{Q_D}) \sum R \\
&-\frac{1}{\omega C_A} - \frac{1}{\omega C_B} - \frac{1}{\omega C_D} + \omega L = (\omega R_B C_B + \omega R_D C_D)(R_A + R_B + R_D) \\
&-\frac{1}{\omega C} + \omega L = (\omega R_B C_B + \omega R_D C_D)(R_A + R_B + R_D) \\
&\frac{\frac{\omega^2}{\omega_0^2} - 1}{\omega C} = (\omega R_B C_B + \omega R_D C_D)(R_A + R_B + R_D) \\
&\omega^2 = \omega_0^2 (1 + \omega C(\omega R_B C_B + \omega R_D C_D)(R_A + R_B + R_D)) \qquad \text{(A.3)} \\
&\omega^2 = \frac{1}{LC}(1 + \frac{1}{L}(R_B C_B + R_D C_D)(R_A + R_B + R_D)) \\
&\omega^2 = \frac{1}{LC}\frac{(L + (R_B C_B + R_D C_D)(R_L + R_B + R_D))}{L} \\
&\omega = \sqrt{\frac{1}{LC}}\sqrt{\frac{L + 2C_{BD} R_{BD} R_L)}{L}} \\
&\omega = \sqrt{\frac{1}{LC}}\sqrt{\frac{L + 2C R_C R_L)}{L}}
\end{aligned}
$$

A.2.2 Frequency stability

$$
\begin{aligned}
&\frac{\partial \omega}{\partial R_L} = \frac{C_{BD} C R_{BD} \omega_0^3}{\sqrt{\frac{2 C_{BD} R_{BD} R_L}{L} + 1}} \approx C_{BD} C R_{BD} \omega_0^3 \\
&\frac{\partial R_L}{\partial T} = a_{TC,R_L} R_L \\
&f_{TC,R_L} = \frac{\partial \omega}{\partial T} / \omega = \frac{\partial \omega}{\partial R_L} \frac{\partial R_L}{\partial T} / \omega \\
&= a_{TC,R_L} C_{BD} C R_{BD} r_L \omega_0^2 = \frac{C_{BD} R_{BD} a_{TC,R_L} L C \omega_0^3}{Q_L} = \frac{a_{TC,R_L}}{Q_L Q_C} \\
&\frac{\partial \omega}{\partial R_C} = \frac{C_{BD} C R_L \omega_0^3}{\sqrt{\frac{2 C_{BD} R_{BD} R_L}{L} + 1}} \approx C_{BD} C R_L \omega_0^3 \\
&\frac{\partial R_C}{\partial T} = a_{TC,R_C} R_C \\
&f_{TC,R_C} = \frac{\partial \omega}{\partial T} / \omega = \frac{\partial \omega}{\partial R_C} \frac{\partial R_C}{\partial T} / \omega \\
&= a_{TC,R_C} C_{BD} C R_{BD} R_L \omega_0^2 = \frac{C_{BD} R_{BD} a_{TC,R_C} L C \omega_0^3}{Q_L} = \frac{a_{TC,R_C}}{Q_L Q_C} \\
&\frac{\partial \omega}{\partial L} = -\frac{(4 C_{BD} R_L R_{BD} + L) \omega_0}{2 L^2 \sqrt{-\frac{2 C_{BD} R_L R_{BD}}{L} + 1}} = -\frac{L \omega_0}{2 L^2} = -\frac{\omega}{2 L} \\
&\frac{\partial L}{\partial T} = a_{TC,L} L \\
&f_{TC,L} = \frac{\partial \omega}{\partial T} / \omega = \frac{\partial \omega}{\partial L} \frac{\partial L}{\partial T} / \omega = -\frac{a_{TC,L} L}{2 L} = -\frac{a_{TC,L}}{2} \\
&\frac{\partial \omega}{\partial C} = -\frac{L \omega_0^3}{2 \sqrt{\frac{2 C_{BD} R_L R_{BD}}{L} + 1}} \approx -\frac{L \omega_0^3}{2} \\
&\frac{\partial C}{\partial T} = a_{TC,C} C \\
&f_{TC,C} = \frac{\partial \omega}{\partial T} / \omega = \frac{\partial \omega}{\partial C} \frac{\partial C}{\partial T} / \omega = -\frac{a_{TC,C} L C \omega^2}{2} = -\frac{a_{TC,C}}{2}
\end{aligned}
\tag{A.4}
$$

A.3 Cross-coupled $(+Ca)$

A.3.1 Oscillation frequency

$$\sum X = -(\frac{1}{Q_B} + \frac{1}{Q_D}) \sum R$$

$$-\frac{1}{\omega C_A} - \frac{1}{\omega C_D} + \omega L = (\omega R_B C_B + \omega R_D C_D)(R_A + R_B + R_D)$$

$$-\frac{1}{\omega C} + \omega L = -(\frac{R_L}{\omega L} - \omega R_D C_D)(R_C + R_L)$$

$$\frac{\frac{\omega^2}{\omega_0^2} - 1}{\omega C} = -(\frac{R_L}{\omega L} - \omega R_D C_D)(R_C + R_L)$$

$$\omega^2 = \omega_0^2(1 - \omega C(\frac{R_L}{\omega L} - \omega R_D C_D)(R_C + R_L)) \tag{A.5}$$

$$\omega^2 = \frac{1}{LC}(1 - \frac{1}{L}(R_L C - R_D C_D)R_L)$$

$$\omega^2 = \frac{1}{LC}\frac{L - (R_L C - R_C C)R_L}{L}$$

$$\omega = \sqrt{\frac{1}{LC}}\sqrt{\frac{L - (R_L C - R_C C)R_L}{L}}$$

$$\omega = \sqrt{\frac{1}{LC}}\sqrt{\frac{L - CR_L^2}{L}}$$

A.3.2 Frequency stability

$$
\begin{aligned}
&\frac{\partial \omega}{\partial R_L} = -\frac{C^2 R_L \omega_0^3}{\sqrt{\frac{-CR_L^2}{L}+1}} \approx -C^2 R_L \omega_0^3 \\
&\frac{\partial R_L}{\partial T} = a_{TC,R_L} R_L \\
&f_{TC,R_L} = \frac{\partial \omega}{\partial T}/\omega = \frac{\partial \omega}{\partial R_L}\frac{\partial R_L}{\partial T}/\omega \\
&= -a_{TC,R_L} C^2 R_L^2 \omega_0^2 = -\frac{L^2 C^2 a_{TC,R_L} \omega_0^4}{Q_L^2} = -\frac{a_{TC,R_L}}{Q_L^2} \\
&\frac{\partial \omega}{\partial R_C} = \frac{C^2 R_C \omega_0^3}{\sqrt{\frac{CR_C^2-CR_L^2}{L}+1}} \approx C^2 R_C \omega_0^3 \\
&\frac{\partial R_C}{\partial T} = a_{TC,R_C} R_C \\
&f_{TC,R_C} = \frac{\partial \omega}{\partial T}/\omega = \frac{\partial \omega}{\partial R_C}\frac{\partial R_C}{\partial T}/\omega \\
&= a_{TC,R_C} C^2 R_C^2 \omega_0^2 = \frac{a_{TC,R_C}}{Q_C^2} \\
&\frac{\partial \omega}{\partial L} = -\frac{(-2CR_L^2+L)\omega_0}{2L^2\sqrt{-\frac{2CR_L^2}{L}+1}} = -\frac{L\omega_0}{2L^2} = -\frac{\omega}{2L} \\
&\frac{\partial L}{\partial T} = a_{TC,L} L \\
&f_{TC,L} = \frac{\partial \omega}{\partial T}/\omega = \frac{\partial \omega}{\partial L}\frac{\partial L}{\partial T}/\omega = -\frac{a_{TC,L} L}{2L} = -\frac{a_{TC,L}}{2} \\
&\frac{\partial \omega}{\partial C} = -\frac{L\omega_0^3}{2\sqrt{-\frac{CR_L^2}{L}+1}} \approx -\frac{L\omega_0^3}{2} \\
&\frac{\partial C}{\partial T} = a_{TC,C} C \\
&f_{TC,C} = \frac{\partial \omega}{\partial T}/\omega = \frac{\partial \omega}{\partial C}\frac{\partial C}{\partial T}/\omega = -\frac{a_{TC,C} LC\omega^2}{2} = -\frac{a_{TC,C}}{2}
\end{aligned}
\tag{A.6}
$$

A.4 Colpitts $(+Ca)$

A.4.1 New R_A

$$\begin{aligned} R_A &= \frac{R_L\frac{L}{C_A} - R_L\frac{L}{C_A} + R_L\frac{1}{\omega^2 C_A^2}}{R_L^2 + \omega^2 L^2 - 2\frac{L}{C_A} + \frac{1}{\omega^2 C_A^2}} \\ &\approx \frac{R_L}{\omega^4 L^2 C_A^2 - 2\omega^2 L C_A + 1} \approx \frac{R_L}{\frac{C_A^2}{C^2} - 2\frac{C_A}{C} + 1} \\ &= \frac{R_L C^{@}}{C_A - 2C_A C + C^2} = \frac{R_L C^2}{(C_A - C)^2} \end{aligned} \quad \text{(A.7)}$$

A.4.2 New X_A

$$\begin{aligned} X_A &= \frac{-R_L^2\frac{1}{\omega C_A} - \frac{\omega L^2}{C_A} + \frac{L}{\omega C_A^2}}{R_L^2 + \omega^2 L^2 - 2\frac{L}{C_A} + \frac{1}{\omega^2 C_A^2}} \\ &\approx \frac{\omega L - \omega^3 L^2 C_A}{\omega^4 L^2 C_A^2 - 2\omega^2 L C_A + 1} \\ &= \frac{\omega L(1 - \frac{C_A}{C})}{\frac{C_A^2}{C^2} - 2\frac{C_A}{C} + 1} = \frac{\omega L(C^2 - C_A C)}{(C_A - C)^2} = \omega L\frac{C}{(C - C_A)} \end{aligned} \quad \text{(A.8)}$$

A.4.3 New ω_0

$$\begin{aligned} &\sum X = 0 \\ &X_A - \frac{1}{\omega C} = 0 \\ &\frac{\omega L C}{C - C_A} = \frac{1}{\omega C} \\ &\omega^2 L C^2 = C - C_A \\ &\omega_0^2 = \frac{C - C_A}{L C^2} \\ &\omega_0 = \sqrt{\frac{C - C_A}{L C^2}} \\ &\omega_0 = \sqrt{\frac{1}{A_X L C}} \end{aligned} \quad \text{(A.9)}$$

A.4.4 Oscillation frequency

$$
\begin{aligned}
&\sum X = -(\frac{1}{Q_B} + \frac{1}{Q_D}) \sum R \\
&-\frac{1}{\omega C_B} - \frac{1}{\omega C_D} + A_X \omega L = (\omega R_B C_B + \omega R_D C_D)(A_R R_A + R_B + R_D) \\
&-\frac{1}{\omega C} + A_X \omega L = (\omega R_B C_B + \omega R_D C_D)(A_R R_A + R_B + R_D) \\
&\frac{\frac{\omega^2}{\omega_0^2} - 1}{\omega C} = (\omega R_B C_B + \omega R_D C_D)(A_R R_A + R_B + R_D) \\
&\omega^2 = \omega_0^2 (1 + \omega C(\omega R_B C_B + \omega R_D C_D)(A_R R_A + R_B + R_D)) \\
&\omega^2 = \frac{1}{A_X LC}(1 + \frac{1}{A_X L}(R_B C_B + R_D C_D)(R_A + R_B + R_D)) \\
&\omega^2 = \frac{1}{A_X LC} \frac{(A_X L + (R_B C_B + R_D C_D)(R_L + R_B + R_D))}{A_X L} \\
&\omega = \sqrt{\frac{1}{A_X LC}} \sqrt{\frac{A_X L + 2CR_C A_R R_L)}{A_X L}}
\end{aligned}
\tag{A.10}
$$

A.4.5 Frequency stability

$$
\begin{aligned}
&\frac{\partial \omega}{\partial R_L} = \frac{A_R C^2 R_C \omega_0^3}{\sqrt{\frac{2CR_C A_R R_L}{A_X L} + 1}} \approx A_R C^2 R_C \omega_0^3 \\
&\frac{\partial R_L}{\partial T} = a_{TC,R_L} R_L \\
&f_{TC,R_L} = \frac{\partial \omega}{\partial T}/\omega = \frac{\partial \omega}{\partial R_L}\frac{\partial R_L}{\partial T}/\omega \\
&= a_{TC,R_L} A_R C^2 R_C R_L \omega_0^2 = \frac{A_R C R_C a_{TC,R_L} LC\omega_0^3}{Q_L} \\
&= \frac{A_R a_{TC,R_L} LC \frac{1}{A_X LC}}{Q_L Q_C} = \frac{A_R a_{TC,R_L}}{A_X Q_L Q_C} \\
&\frac{\partial \omega}{\partial R_C} = \frac{A_R C^2 R_L \omega_0^3}{\sqrt{\frac{2CR_C A_R R_L}{A_X L} + 1}} \approx A_R C^2 R_L \omega_0^3 \\
&\frac{\partial R_C}{\partial T} = a_{TC,R_C} R_C \\
&f_{TC,R_C} = \frac{\partial \omega}{\partial T}/\omega = \frac{\partial \omega}{\partial R_C}\frac{\partial R_C}{\partial T}/\omega \\
&= a_{TC,R_C} A_R C^2 R_L R_C \omega_0^2 = \frac{A_R C R_C a_{TC,R_C} LC\omega_0^3}{Q_L} = \frac{A_R a_{TC,R_C}}{A_X Q_L Q_C} \\
&\frac{\partial \omega}{\partial L} = \frac{(2CA_R R_C R_L - LA_X) C^2 A_X \omega_0^5}{2\sqrt{-\frac{A_R C R_L R_C}{A_X L} + 1}} = -\frac{LC^2 A_X^2 \omega_0^5}{2} \\
&\frac{\partial L}{\partial T} = a_{TC,L} L \\
&f_{TC,L} = \frac{\partial \omega}{\partial T}/\omega = \frac{\partial \omega}{\partial L}\frac{\partial L}{\partial T}/\omega = -\frac{a_{TC,L} L^2 C^2 A_X^2 \omega_0^4}{2} = -\frac{a_{TC,L}}{2} \\
&\frac{\partial \omega}{\partial C} = -\frac{L\omega_0 \frac{1}{LC}}{2\sqrt{\frac{2C^2 R_C + 2CR_C A_R}{A_X L} + 1}} \approx -\frac{L\omega_0 \frac{1}{LC}}{2} \\
&\frac{\partial C}{\partial T} = a_{TC,C} C \\
&f_{TC,C} = \frac{\partial \omega}{\partial T}/\omega = \frac{\partial \omega}{\partial C}\frac{\partial C}{\partial T}/\omega = -\frac{a_{TC,C} LC \frac{1}{LC}}{2} = -\frac{a_{TC,C}}{2}
\end{aligned}
\tag{A.11}
$$

A.4.6 Unsimplified A_X

$$
\begin{aligned}
A_X &= \frac{-R_L^2 \frac{1}{\omega^2 L C_A} - \frac{\omega L}{C_A} + \frac{1}{\omega C_A^2}}{R_L^2 + \omega^2 L^2 - 2\frac{L}{C_A} + \frac{1}{\omega^2 C_A^2}} \\
&= \frac{-R_L^2 \frac{C_A}{L} - \omega^2 C_A L_A + 1}{R_L^2 \omega^2 C_A^2 + \omega^4 L^2 C_A^2 - 2\omega^2 L C_A + 1} \\
&= \frac{-R_L^2 \frac{C_A}{L} - \frac{C_A}{A_X C} + 1}{\frac{R_L^2 C_A^2}{A_X L C} + \frac{C_A^2}{C^2 A_X^2} - 2\frac{C_A}{C A_X} + 1} \\
&= \frac{-R_L^2 C^4 C_A - C_A L C^2 (C - C_A) + L C^4}{C^2 C_A^2 R_L^2 (C - C_A) + L C_A^2 (C - C_A)^2 - 2 L C_A C^2 (C - C_A) + L C^4}
\end{aligned}
\tag{A.12}
$$

A.4.7 Frequency stability for A_X

$$
\begin{aligned}
&\frac{\partial \omega}{\partial A_X} = -\frac{C^2 L \omega^5 (4 A_R R_C C R_L + L A_X)}{2\sqrt{\frac{2 A_R R_C C R_L}{L A_X} + 1}} \approx \\
&-\frac{A_X C^2 L^2 \omega^5}{2} = -\frac{\omega}{2 A_X} \\
&\frac{\partial A_x}{\partial R_L} = -\frac{2 C_A C^4 R_L (C_A - C)(2C_A^2 - 2C_A C + C^2)(C_A^2 - C_A C + C^2)}{L(C - C_A)(C_A^2 - C_A C + C^2)^4} \\
&= -\frac{2 C_A C^4 R_L (C_A - C)(2C_A^2 - 2C_A C + C^2)}{L(C - C_A)(C_A^2 - C_A C + C^2)^3} \\
&\frac{\partial R_L}{\partial T} = a_{TC,R_L} R_L \\
&f_{TC,A_X} = \frac{\partial \omega}{\partial T}/\omega = \frac{\partial \omega}{\partial A_X}\frac{\partial A_X}{\partial R_L}\frac{\partial R_L}{\partial T}/\omega \\
&= \frac{2 a_{TC,R_L} C_A C^3 R_L^2 (C_A - C)(2C_A^2 - 2C_A C + C^2)}{L(C_A^2 - C_A C + C^2)^3}
\end{aligned}
\tag{A.13}
$$

A.5 Colpitts $(Qc = 54.3)$

A.5.1 Q-factor compensation

$$
\begin{aligned}
& f_{TC,R_L} + f_{TC,R_C} + f_{TC,L} + f_{TC,C} = 0 \\
& \frac{a_{TC,R_L}}{Q_L Q_C} + \frac{a_{TC,R_C}}{Q_L Q_C} - \frac{a_{TC,L}}{2} - \frac{a_{TC,C}}{2} = 0 \\
& \frac{a_{TC,R_L}}{Q_L Q_C} + \frac{a_{TC,R_C}}{Q_L Q_C} = \frac{a_{TC,L}}{2} + \frac{a_{TC,C}}{2} \\
& Q_L = \frac{2(a_{TC,R_L} + a_{TC,R_C})}{Q_C(a_{TC,L} + a_{TC,C})} \\
& Q_C = \frac{2(a_{TC,R_L} + a_{TC,R_C})}{Q_L(a_{TC,L} + a_{TC,C})}
\end{aligned}
\tag{A.14}
$$

Appendix B

Schematics and parameter tables

This part of the Appendix includes supporting schematics and parameter tables

B.0.1 Schematics

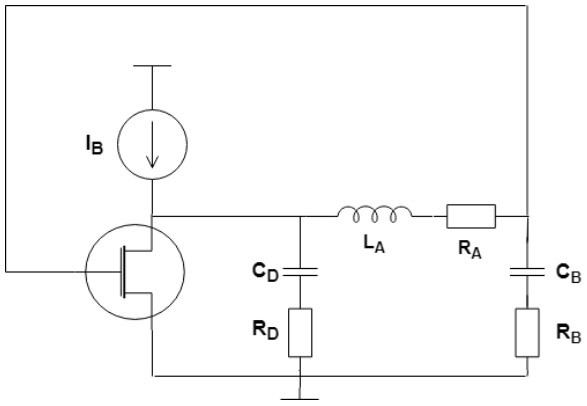

Figure B.1: Colpitts common-gate schematic

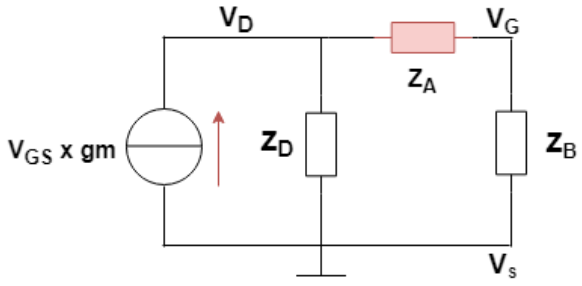

Figure B.2: Cross-coupled simplified schematic

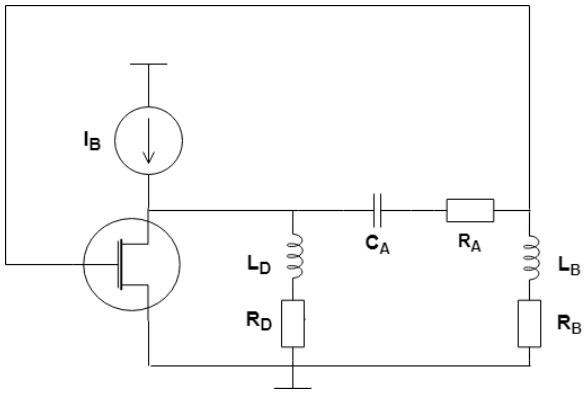

Figure B.3: Hartley schematic

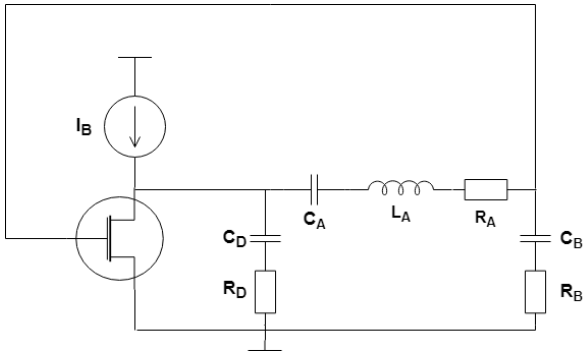

Figure B.4: Clapp schematic

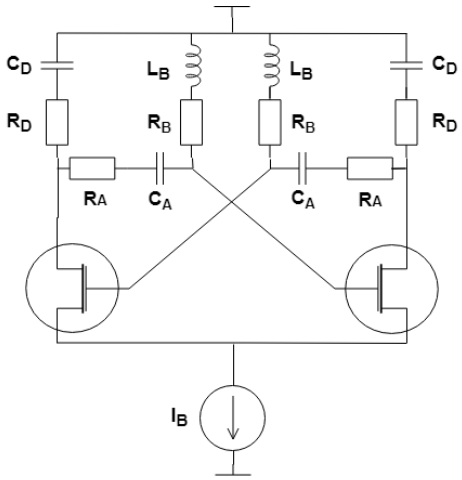

Figure B.5: Cross-coupled $(+Ca)$ schematic

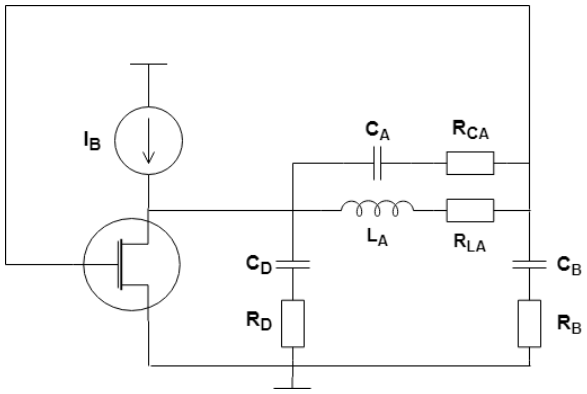

Figure B.6: Colpitts $(+Ca)$ schematic

B.0.2 Parameter tables

Table B.1: Parameter ranges and values

	L	**C**	**frequency**
range	$0.5 - 5nH$	$100fF - 20pF$	$1 - 2GHz$
Q	10	200	

Table B.2: Temperature coefficients

	a_{TC,R_L}	a_{TC,R_C}	$a_{TC,L}$	$a_{TC,C}$
value	4000	4000	15	15